Soldagem & Inspeção. 2018;23(1):32-42
https://doi.org/10.1590/0104-9224/SI2301.04
ISSN 1980-6973 (Online)
ISSN 0104-9224 (Print)

Influence of the Aluminium Alloy Type on Defects Formation in Friction Stir Lap Welding of Thin Sheets

M. I. Costa[1], C. Leitao[1], D. M. Rodrigues[2]

[1] Universidade de Coimbra – UC, Centro de Engenharia Mecânica, Materiais e Processos – CEMMPRE, Departamento de Engenharia Mecânica, Coimbra, Portugal.
[2] Universidade de Coimbra – UC, Instituto para a Sustentabilidade e Inovação em Engenharia Estrutural – ISISE, Departamento de Engenharia Mecânica, Coimbra, Portugal.

Received: 23 Jan., 2018
Accepted: 07 Mar., 2018

E-mail: carlos.leitao@dem.uc.pt (CL)

Abstract: The weldability in Friction Stir Lap Welding (*FSLW*) of heat and non-heat treatable aluminium alloys, the AA6082-T6 and the AA5754-H22 aluminium alloys, respectively, are compared. For both alloys, welds were produced in very thin sheets, using the same welding parameters and procedures, and strong differences in welds morphology were found. The strength of the welds was evaluated by performing tensile-shear tests under monotonic and cyclic loading conditions. As-welded and heat-treated samples of the AA6082- T6 were tested. It was found that the heat-treatable alloy is more sensitive to defects formation, in lap welding, than the non-heat-treatable alloy. The presence of defects has a strong influence on the monotonic and fatigue behaviour of the welds. In spite of this, for very high-applied stresses, the heat-treatable alloy welds perform better in fatigue than the non-heat-treatable alloy welds.

Key-words: FSW; Weldability; Aluminium alloys; Defects; DIC.

Influência do Tipo de Liga de Alumínio na Formação de Defeitos em Soldaduras em Chapas Finas Unidas por *Friction Stir Lap Welding*

Resumo: No presente trabalho são comparadas as soldabilidades de duas ligas de alumínio: a liga AA6082-T6, tratável termicamente, e a liga AA5754-H22, não-tratável termicamente. Foram produzidas soldaduras, em chapas finas, pelo processo *Friction Stir Lap Welding* (*FSLW*). Concluiu-se que apesar da utilização dos mesmos parâmetros e procedimentos de soldadura, as soldaduras produzidas nas duas ligas apresentavam diferenças morfológicas consideráveis. A resistência mecânica das soldaduras foi avaliada através da realização de ensaios de tração e de fadiga. Por se tratar de uma liga tratável termicamente, as soldaduras produzidas na liga AA6082-T6 foram também testadas após tratamento térmico. Concluiu-se que a liga tratável termicamente tem maior propensão para a formação de defeitos, na ligação em junta sobreposta, do que a não-tratável termicamente. A presença de defeitos tem uma grande influência no comportamento das soldaduras, nos ensaios de tração e fadiga. Observou-se que, para as cargas de solicitação mais elevadas, a liga tratável termicamente apresentou uma maior resistência à fadiga do que a não-tratável termicamente.

Palavras-chave: FSW; Soldabilidade; Ligas de alumínio; Defeitos; DIC.

1. Introduction

Studies on the Friction Stir Welding (*FSW*) of aluminium alloys are abundant in recent literature attending to the relatively short life of the technology and to the very wide range of applications envisaged worldwide [1]. However, despite the diversity of the investigation performed, systematised information on particular base materials weldability, or comparative analysis on the weldability of different alloys of the same family, is still hard to find. Leitão et al. [2], for example, compared the friction stir weldability of heat-treated and non-heat-treated aluminium alloys, using butt welds produced in 3 and 6 mm thick plates. The authors found that the heat-treatable alloy had superior weldability in *FSW* than the non-heat-treatable alloy and stated that the important differences in weldability, between the two alloys, were related to the important differences in plastic behaviour, at high temperatures and strain rates, of both base materials. Leitão et al. [3] also analysed the influence of the base materials plastic properties on the welding thermo-mechanisms, assessed by performing a torque sensitivity analysis.

An important influence of base materials plastic properties, on welds characteristics, was also depicted by Galvão et al. [4], in dissimilar lap welding of copper and aluminium, and by Costa et al. [5], in dissimilar lap welding of aluminium alloys. In both studies, heat and non-heat treatable aluminium alloys were matched in different combinations of Al-Cu and Al-Al welds. According to Galvão et al. [4], the welds produced combining a non-heat-treatable aluminium alloy with copper, presented good surface finishing and defective joint interface, meanwhile the welds produced combining a heat-treatable aluminium alloy with copper, presented a poor quality surface finishing and effective base materials mixing at the joint interface. In this study, the copper plates were always positioned on the top of the joint, in contact with the *FSW* tool. Costa et al. [5] analysed the influence of the plates relative positioning in dissimilar aluminium lap welding. The authors report that the welds produced with the heat-treatable alloy on the top of the joint displayed higher strength than the welds produced with the reverse base materials positioning. The differences in the dissimilar weld's strength were explained by the influence of the base materials plastic behaviour, at high temperature, on lap welds defects formation.

In Friction Stir Lap Welding (*FSLW*), hooking and cold-lap defects are usual and were found to have a significant impact on joints strength for a large range of ferrous and non-ferrous base materials. Cederqvist and Reynolds [6] were the first to report the presence of these defects, at the advancing and retreating sides, respectively, of dissimilar AA2024-AA7075 lap welds. Since Cederqvist and Reynolds [6] pioneer work, a large range of results on the evolution of lap defects size, shape and location, may be found in *FSLW* literature, which may be attributed the large variety of tools, base materials and process parameters tested. Ericsson et al. [7] claimed that using a tool with a convex pin end induced severe hooking defects in AA6082 aluminium alloy welding. Fadeifard et al. [8] showed that a subconical pin-head induced the formation of a hooking defect in the bottom sheet, in AA6061 aluminium alloy welding. Salari et al. [9] claimed that the use of a conical-cylindrical pin might diminish the severity of the lap welding defects when compared to other pin geometries, during welding of AA5456 aluminium alloys. Salari et al. [10] corroborated these conclusions and added that controlling the heat input, through an appropriate choice of process parameters, enables to improve the base material stirring across the lap interface. Shirazi et al. [11] proved that not only the pin length, but also, the interaction between the pin threads and the tool rotation direction, influence the hook and/or cold lap defects formation.

The tool rotational (ω) and traverse (*v*) speeds were also found to have a strong influence on defects formation. Yadava et al. [12] proved that the hook and the cold lap defects increased with increasing process pitch, i.e., the v/ω ratio. Chen and Yazdanian [13] showed that the hook size increased when increasing the tool rotational speed, in AA6060 aluminium alloy welding. In Yazdanian et al. [14] is shown that increasing the rotational speed, or decreasing the tool traverse speed, increases the defect's size. Liu et al. [15], on the other hand, found that the defect's size decreased with increasing welding speeds in AA6005 aluminium alloy welding.

According to the authors cited in the previous paragraphs, the formation of the lap welding defects can be mitigated by optimising the welding parameters and/or by properly selecting the tool geometry. Only Costa et al. [5] reported a strong influence of base materials positioning/properties on defects formation in dissimilar aluminium lap welding. In current work, a set of similar welds selected from Costa et al. [16] and Costa et al. [17], is compared to assess the influence of base materials properties on defects formation in lap welding of thin sheets. AA 6xxx and AA 5xxx aluminium alloys were used in the investigation, due to its importance and wide use in the transportation industries [18,19].

2. Experimental Procedure

The weldability in *FSLW* of the heat and non-heat treatable alloys will be compared by analysing similar lap welds produced in 1 mm thick plates of the AA6082-T6 (Al-Mg-Si) and AA5754-H22 (Al-Mg) alloys. From Table 1, where are compared the tensile properties, at room temperature, for both base materials, it is possible to conclude that the AA6082-T6 alloy displays much higher yield and tensile strength than the AA5754-H22 alloy.

Table 1. Base materials mechanical properties.

Material	*Yield Strength* [MPa]	*Ultimate Tensile Strength* [MPa]
AA5754 (Non-heat treatable)	170	276
AA6082 (Heat treatable)	300	399

All the welds were produced using an MTS I-STIR PDS equipment. The welding parameters used to produce the welds are described in Table 2. The H13 steel tool geometry is shown in Figure 1. As shown in the table, only the welding speeds were varied, from 350 to 1000 mm/min. Along the text, the welds will be labelled according to the base material, and the welding speed used in each test, i.e., the AA6082 weld produced at 350 mm/min will be labelled 6_350.

Table 2. Welding parameters.

Weld	Material	Rotational speed, ω [rpm]	Welding speed, *v* [mm/min]	Tilt angle [°]	Plunge depth, *dz* [mm]
6_350	AA6082	600	350	2	1.2
6_700			700		
6_1000			1000		
5_350	AA5754	600	350	2	1.2
5_700			700		
5_1000			1000		

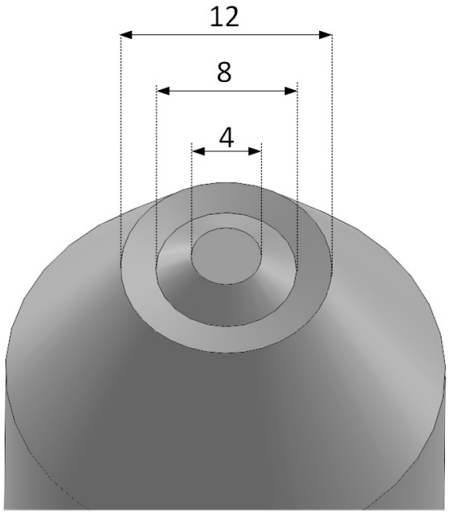

Figure 1. FSW tool geometry (dimensions in mm).

For the morphological and metallographic analysis, transverse specimens of all the welds were cut, cold mounted, polished, etched with modified Poulton's reagent and observed with a Leica DM4000M LED optical microscope.

The mechanical strength of the welds was evaluated by performing transverse-tensile and tensile-shear tests in an Instron 4206 universal testing machine. The geometry of the specimens is shown in Figure 2. The tensile-shear tests were performed using advancing (*AS*) and retreating (*RS*) side loading modes. During testing, the GOM Aramis 5M system was used for strain data acquisition by Digital Image Correlation (*DIC*). Local stress-strain curves, for different weld zones, were plotted following the practices described in Leitão et al. [20, 21]. The fatigue strength of the welds was evaluated in tensile-shear loading with a 10 Hz frequency, a stress ratio of 0.01 and stress ranges varying from 30 to 150 MPa. The fatigue tests were performed using an Instron Electro Plus E10000 machine. At least three samples of each weld were tested, in all testing conditions, in order to check the reproducibility of the results.

Finally, some AA6082 welds were subjected to a post-weld heat treatment (*PWHT*) to homogenise the mechanical properties along the welds cross-section. The *PWHT* comprised an initial solubilisation, at 535°C, during 2 hours, followed by artificial ageing, at 175ºC, during 8 hours. In the text, the samples of the welds tested after *PWHT* will be identified with the suffix AH. The samples of the welds tested in the as-welded condition will be identified with the suffix AW.

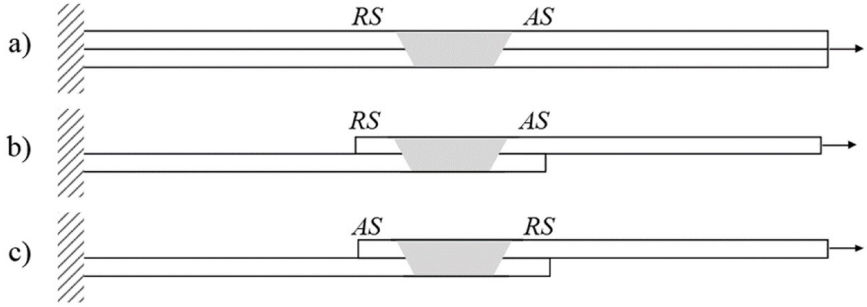

Figure 2. Transverse-tensile (a) and AS (b) and RS (c) tensile-shear samples [17].

3. Results

3.1. Morphological analysis of the welds

In Figure 3 are compared the welds produced in both base materials at the lowest and highest welding speeds tested in current work, i.e., 350 and 1000 mm/min. No important defects or differences in surface morphology can be depicted when comparing the welds produced in the two different base materials using similar process parameters. However, in spite of the strong similarities in surface quality, strong differences in the cross-section morphology were depicted. The images in Figure 3, for example, enable to observe important differences in the Effective Joint Width (*EJW*), i.e., the width of the connected interface between the two plates.

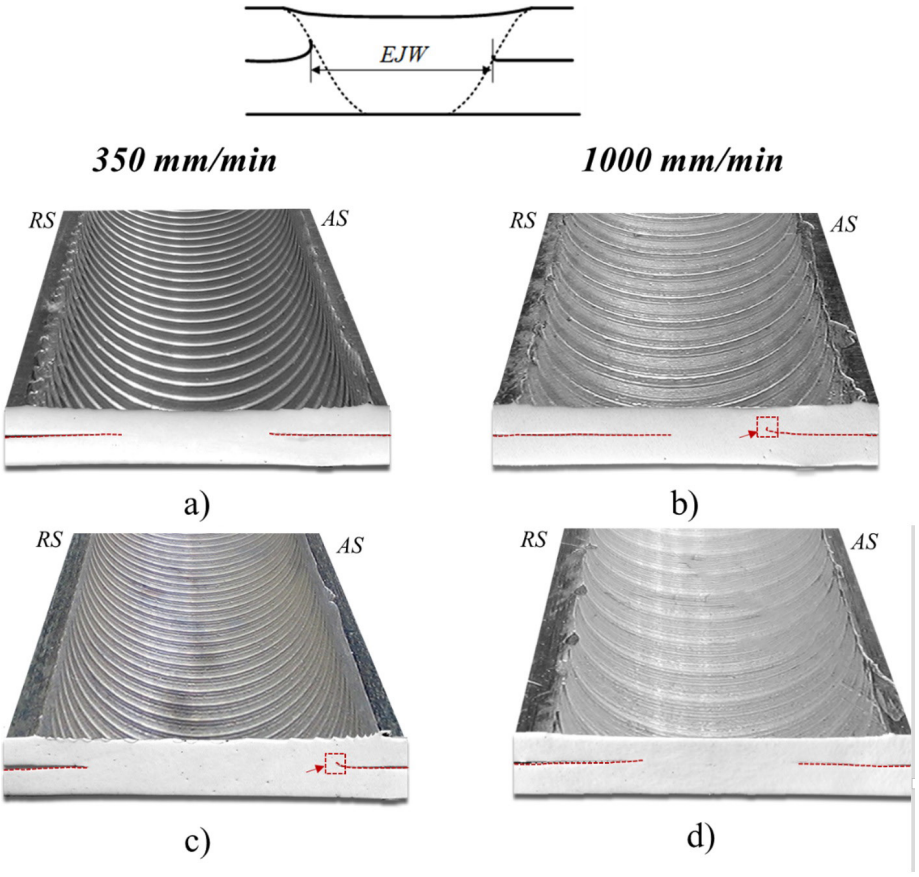

Figure 3. Surface and cross-section morphologies of the 5_350AH (a), 5_1000 (b), 6_350AH (c) and 6_1000 (d) welds.

The evolution of the Effective Joint Width with the welding speed, for both base materials, is plotted in Figure 4. Analysing the results it is possible to conclude that, independently of the welding speed, the *EJW* was always larger for the AA6082 welds than for the AA5754 welds. For both base materials, the *EJW* decreased when increasing the welding speed. However, for the AA5754 alloy, the decrease in the *EJW* was much steeper than for the AA6082 alloy.

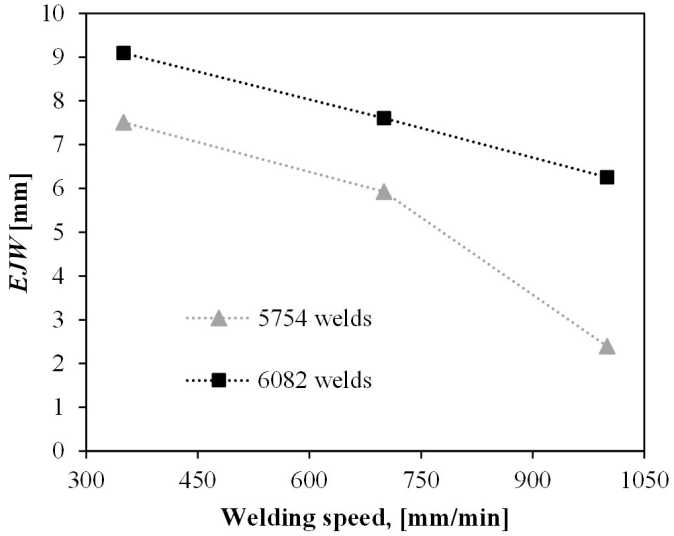

Figure 4. Evolution of the effective joint width with the welding speed.

The important differences in *EJW*, between the welds produced in the AA6082 and AA5754 alloys, indicate that the bonding, which results from the stirring of the base materials at the plates interface, was more effective for the heat-treatable alloy. Leitão et al. [2], who also observed important differences in cross-section morphology between heat and non-heat treatable aluminium alloys butt welds, state that at very high temperatures, the AA6xxx alloys experiences higher softening than the AA5xxx alloys, which enables a more effective material stirring during welding. So, during *FSLW*, under the same loading conditions, the AA6082 would have experienced more intense plastic deformation than the AA5754 alloy, which contributed to a more effective bonding between the plates and larger *EJW*s.

The formation of a hooking defect, of very small size, at the advancing side of the 6_350 and 5_1000 welds, is also visible in Figure 3. No cold lap defects can be depicted in any of the cross-sections. However, observing and measuring these two types of defects in the cross-sections of the welds is not always easy. For this reason, in current work, the severity of the lap welding defects will be assessed using the mechanical testing results, more precisely, maps of the strain distribution in samples tested in monotonic loading.

3.2. Mechanical characterization

3.2.1. Monotonic loading

According to the practices followed in Costa et al. [16], the yield strength of the joints in tensile-shear loading was related to that of the base material, by calculating the Normalized Yield Load (*NYL*) parameter, using Equation 1:

$$NYL = \frac{F_{yield}^{weld}}{F_{yield}^{bm}} \quad (1)$$

In this equation, F_{yield}^{weld} correspond to the yield load registered in the tensile-shear testing of the advancing and retreating side samples, and F_{yield}^{bm} correspond to the yield load of the base material, registered in the uniaxial tensile testing of samples of the same width of the tensile-shear samples.

In Figures 5a and 5b are compared the evolution of the advancing and retreating sides *NYLs*, respectively, with the welding speed, for the AA5754 alloy and for the AW and AH samples of the AA6082 alloy. From the figures it is possible to conclude that meanwhile the AA5754 joints had advancing and retreating side yield strengths similar to that of the base material (*NYL*≈1), the AA6082AW welds had yield strength much lower than that of the base material (*NYL*<<1), for both loading modes. Contrary to that registered for the AA5754 welds, the advancing and retreating side strengths were very different for the AA6082AW welds. The advancing side strength increased, and the retreating side strength decreased, when increasing the welding speed. In spite of this, the retreating side strength was always higher than the advancing side strength.

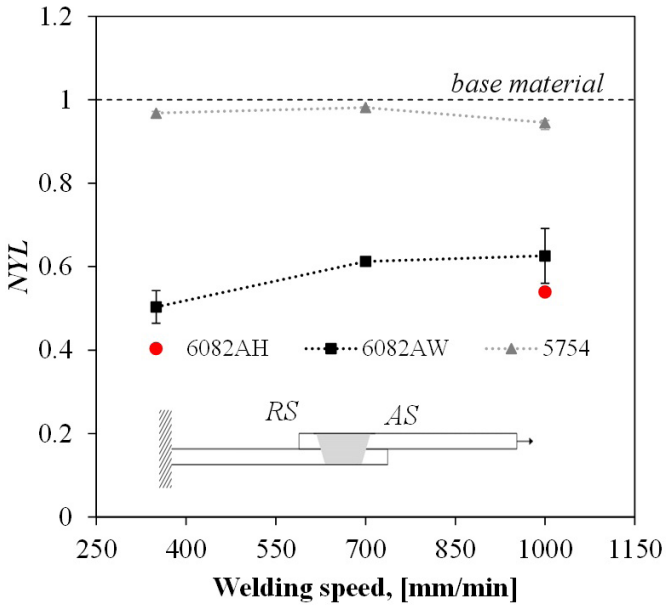

(a)

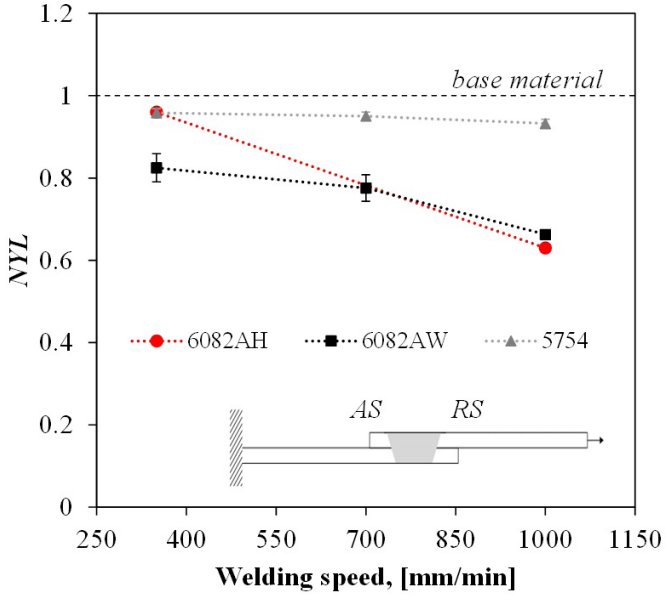

(b)

Figure 5. NYL vs welding speed for AS (a) and RS (b) samples testing.

Meanwhile, the high tensile-shear strength efficiency of the AA5754 welds may be related to the absence of welding defects, the important under-match in tensile-shear strength between the AA6082AW welds, and the base material, is for sure related to the softening occurring when welding this alloy. The mechanisms of material softening in *FSW* of AA6XXX alloys are well explained in Sato et al. [22]. The unsymmetrical evolution of the advancing and retreating side yield strengths, with the welding speed, may be associated with two phenomena: (1) the variation of the strength of the welds with the welding speed and/or (2) the presence of important weld defects at the advancing and retreating sides of the AA6082 welds.

The weld material strength was evaluated by testing transverse-tensile samples (Figure 2a) of all the welds. Using the procedures detailed in Leitão et al. [20], local true stress-strain curves were plotted. In Figure 6 the local stress-strain curves for the Thermomechanical Affect Zone (*TMAZ*) of the welds performed at welding speeds of 350 mm/min and 1000 mm/min, in the as-welded and age-hardened conditions, are compared with those of each base material. The graph shows that both alloys experienced softening in the *TMAZ* during *FSW*. However, as expected, in the as-welded condition, the under-match in *TMAZ* yield strength, relative to the base material, was much higher for the heat-treatable (AA6082) than for the non-heat-treatable (AA5754) alloy. In fact, for the AA6082 alloy, the *TMAZ* softening was a result of the dissolution and coarsening of the strengthening precipitates, as explained by Sato et al. [22], while for the AA5754 alloy, the *TMAZ* softening resulted from the recovery of the strain-hardened structure of the base material, as explained by Bozkurt et al. [23]. By performing the *PWHT*, the strength of the base material was partially recovered in the *TMAZ* of the heat-treatable alloy, as can be concluded by analysing the results relative to the AH samples.

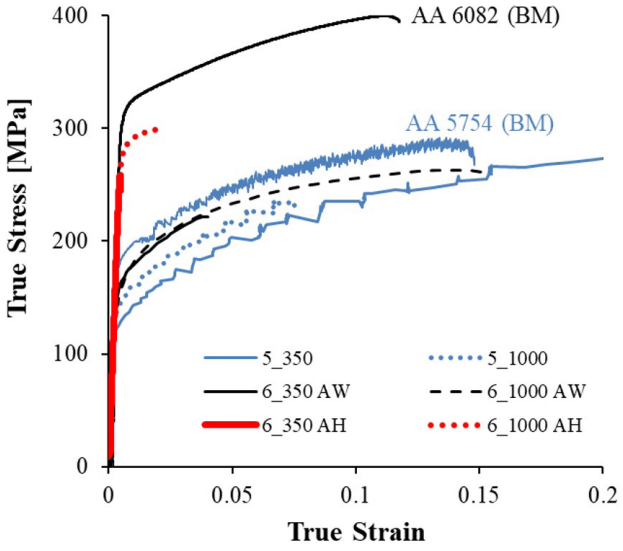

Figure 6. Tensile curves of the transverse-tensile samples of welds produced at 350 and 1000 mm/min using both base materials.

Figure 6 also shows that, for each aluminium alloy, no important differences in the local strength of the TMAZ were registered when testing the welds produced with the different welding speeds. This way, the significant differences in tensile-shear strength between the AA6082 welds (Figure 5) cannot be related to differences in the local strength of the TMAZ, but have to be related to the presence of welding defects, with varying severity, at the advancing and retreating sides of the joints.

According to Costa et al. [5], for the AA6082 alloy, which displays intense flow softening during plastic deformation at high temperatures, the material of the lower plate easily flows upward, under the axial load exerted by the FSW tool, giving rise to important defects at both the advancing and retreating sides of the welds. Contrarily, the AA5754 alloy, which displays perfect plastic behaviour at high temperatures, does not experience intense flow softening during the plastic deformation imposed by the FSW tool. Consequently, de material of the lower plate

does not flow upward, so easily as for the AA6082 alloy, hindering the formation of those defects. Leitão et al. [2] discuss the softening mechanisms during the plastic deformation at high temperatures of the AA6082 alloy, relating it to the improved flow of this material in FSW. According to these authors, in butt welding, the AA6XXX alloys are less sensitive to welding defects formation than the AA5xxx alloys. In lap welding, the improved flowability of the AA6xxx alloys, explain the higher values of the *EJW* registered in Figure 4, for the AA6082 welds, but also explain the formation of important welding defects, with a deleterious effect on the joints performance, displayed in Figure 5.

In order to support the previous conclusions concerning the presence of important defects in the AA6082 welds, in Figure 7a and Figure 7b are compared the Mises strain distributions, in the top plate of advancing and retreating samples, respectively, of both base materials, at maximum load. As shown in the figure, independently of the base material, the tensile-shear samples failure occurred in the top plate, at the boundary between the connected and unconnected interfaces of the lap plates. However, meanwhile most of the AA5754 samples had rupture after the base material was plastically deformed, the AA6082AW samples had rupture with no plastic deformation in the base material. Actually, for the AA6082AW samples, plastic deformation was only noticeable for the retreating side samples, in the failure region, which is located inside the softened *TMAZ-HAZ* interface [17].

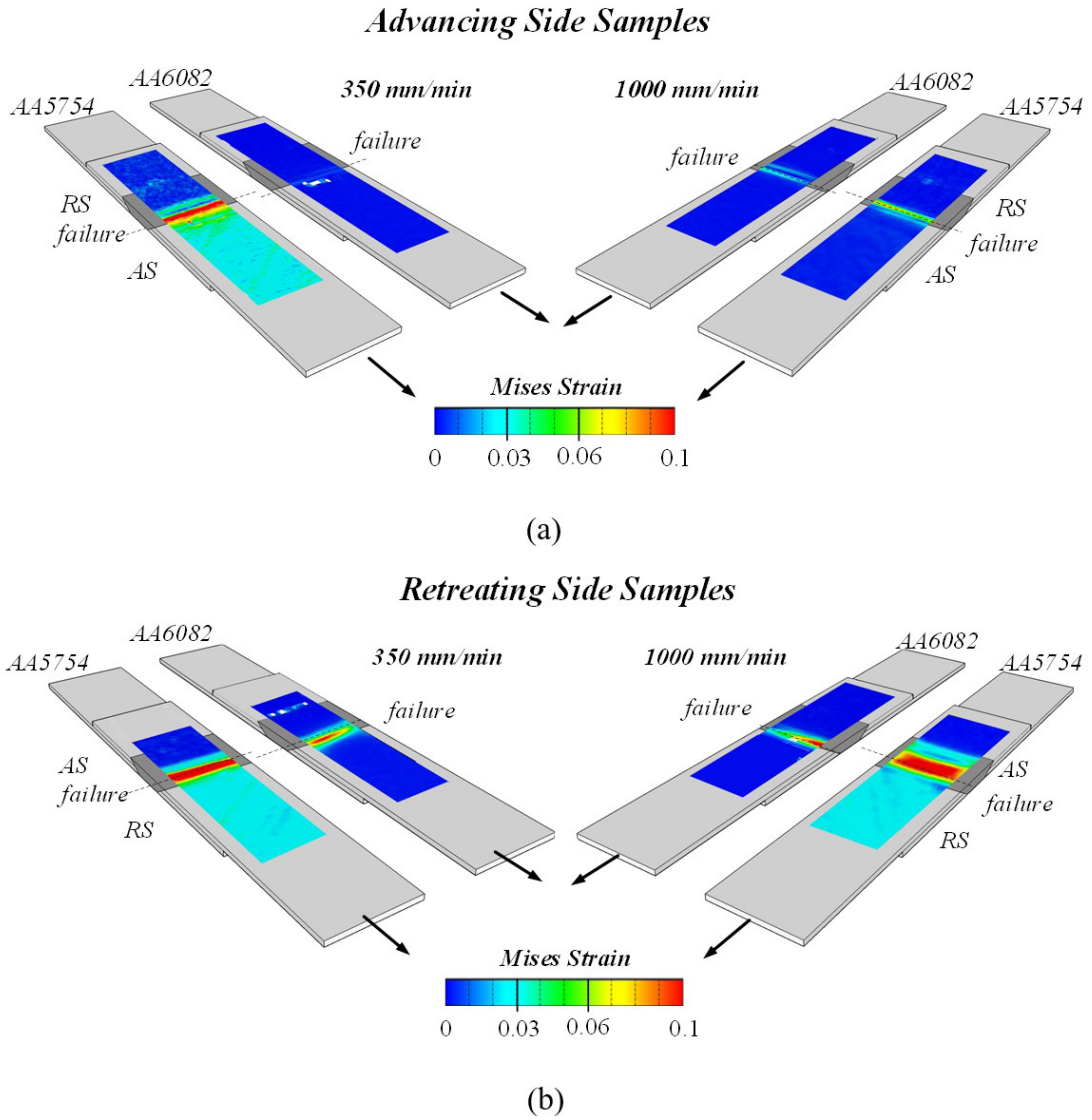

Figure 7. Strain distribution, at the maximum load, for AS (a) and RS (b) samples of the welds performed at 350mm/min and 1000 mm/min.

The strain distribution maps in Figure 7 are also illustrative of the absence of important welding defects acting as stress concentrators for most of the AA5754 welds. The only exception was registered for the 5_1000 weld, for which the advancing side sample had rupture without plastic deformation in the base material. For the AA6082AW welds, on the other hand, all the advancing and retreating side samples had rupture for very small plastic deformation values, in spite of the base material softening in the weld region. These results corroborate the previous hypothesis of the presence of important defects at the advancing and retreating sides of these welds.

In order to exclude the effect of the softening on the strength of the AA6082 welds, some samples of welds produced at 350 mm/min and 1000 mm/min were subjected to *PWHT*. In Figure 5 are shown the *NYL*s for the AA6082AH welds. For the welds produced at 350 mm/min only retreating side samples were tested in the age-hardened condition, due to the very low advancing side strength of this weld in the as-welded condition. The graph shows that after the PWHT, only the retreating side samples of the 6_350AH welds displayed yield strength similar to that of the base material, indicating the absence of defects. For the 6_1000AH welds, the strength was not significantly improved by the *PWHT*, proving the presence of severe defects at both the advancing and retreating sides. In Figure 8 are compared the strain distribution maps, at maximum load, for retreating side samples of the AA5754 welds and AA6082AH welds. The images show that after post-welding heat-treatment, the strain distribution for the 6_350AH retreating side samples become similar to that of the 5_350 samples. On the other hand, for the 6_1000AH welds, with severe retreating side defects, the rupture occurred before any plastic deformation took place in the samples. Actually, due to the severity of the defects, even the transverse-tensile samples of the AA6082AH welds failed for very small values of elongation, as it is possible to depict by the stress-strain curves in Figure 6.

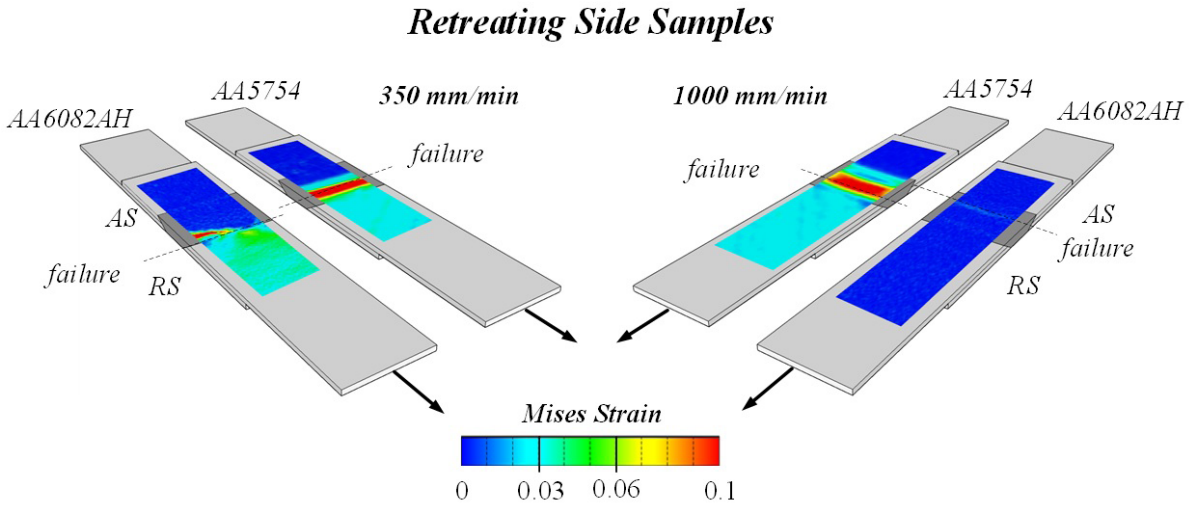

Figure 8. Strain distribution maps in RS samples of welds produced at 350 and 1000 mm/min, for AA5754 welds and the AA6082 welds in the age-hardened condition.

3.2.2. Cyclic loading

Fatigue tests were performed using tensile-shear retreating side samples. According to the results shown in Figure 5, these samples displayed the best performance in the monotonic tests. For the AA6082 alloy, only the results from the 6_350 weld are displayed, since the monotonic tests showed that this weld was the one with the higher strength. For the AA5754 alloy, only samples of the 5_1000 weld were tested. According to Figure 5, all the welds produced in this alloy had similar strength. In this way, it was tested the sample of the weld produced at higher welding speed, which is the most interesting in terms of process productivity [16]. In Figure 9 are compared the S-N curves for both alloys. In the graph, the fatigue load was normalized relative to the yield stress of the *TMAZ* material, determined using the local stress-strain curves in Figure 6. The fatigue test results show that, for the

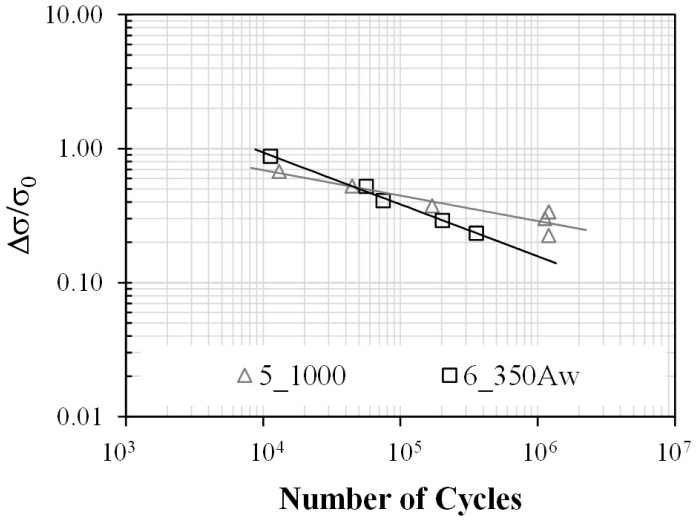

Figure 9. Fatigue tests results.

lowest fatigue loads tested in current work, the AA6082 weld had lower fatigue strength than the AA5754 weld. In spite of this, for the higher testing loads, the 6_350AW weld had higher fatigue strength than the 5_1000 weld. According to Costa et al. [17], the presence of a softer material in the *TMAZ* contributes to improve the fatigue strength of the AA6082 joints. So, it is reasonable to assume that the lower fatigue strength of the 6_350AW weld, relative to the 5_1000 weld, at very low loads, is related to lower quality of the connection. More precisely, at the highest load values, for which plastic deformation takes place at the unconnected tip of the lap joint, the protective effect of the soft *TMAZ* on the joint performance contributed to improve the fatigue strength of the 6_350AW weld to values close to that of the 5_1000 weld. As shown in Costa et al. [17], by performing *PWHT*, the fatigue strength of the AA6082 welds is decreased.

4. Conclusions

- The heat-treatable alloy is more sensitive to defects formation, than the non-heat-treatable alloy, in lap welding;
- Due to the formation of welding defects, the heat-treatable alloy welds display strong asymmetry in weld properties, in advancing and retreating side loading;
- The non-heat-treatable alloy welds, absent of important welding defects, display symmetry in weld properties;
- The strength of the lap joints does not depend on the effective joint width (*EJW*) between the two plates, but on the presence of welding defects at the advancing and/or retreating sides of the joints.

Acknowledgements

This research was co-financed through Fundação para a Ciência e a Tecnologia (UID/EMS/00285/2013) and COMPETE 2020 - Programa Operacional Competitividade e Internacionalização (POCI-01-0145-FEDER-007633) projects. The authors, C. Leitão and M.I. Costa, are supported by the Portuguese Foundation for Science and Technology through SFRH/BPD/93685/2013 and SFRH/BD/104073/2014 fellowships, respectively. All supports are gratefully acknowledged.

References

[1] Magalhães VM, Leitão C, Rodrigues DM. Friction stir welding industrialisation and research status. Science and Technology of Welding and Joining. 2017;1-10. http://dx.doi.org/10.1080/13621718.2017.1403110.

[2] Leitão C, Louro R, Rodrigues DM. Analysis of high temperature plastic behaviour and its relation with weldability in friction stir welding for aluminium alloys AA5083-H111 and AA6082-T6. Materials & Design. 2012;37:402-409. http://dx.doi.org/10.1016/j.matdes.2012.01.031.

[3] Leitão C, Louro R, Rodrigues DM. Using torque sensitivity analysis in accessing Friction Stir Welding/Processing conditions. Journal of Materials Processing Technology. 2012;212(10):2051-2057. http://dx.doi.org/10.1016/j.jmatprotec.2012.05.009.

[4] Galvão I, Verdera D, Gesto D, Loureiro A, Rodrigues DM. Influence of aluminium alloy type on dissimilar friction stir lap welding of aluminium to copper. Journal of Materials Processing Technology. 2013;213(11):1920-1928. http://dx.doi.org/10.1016/j.jmatprotec.2013.05.004.

[5] Costa MI, Verdera D, Leitão C, Rodrigues DM. Dissimilar friction stir lap welding of AA 5754-H22 / AA 6082-T6 aluminium alloys: In fl uence of material properties and tool geometry on weld strength. Materials & Design. 2015;87:721-731. http://dx.doi.org/10.1016/j.matdes.2015.08.066.

[6] Cederqvist L, Reynolds AP. Factors affecting the properties of friction stir welded aluminum lap joints. Welding Journal. 2001;80:281-287.

[7] Ericsson M, Jin L, Sandstrom R. Fatigue properties of friction stir overlap welds. International Journal of Fatigue. 2007;29(1):57-68. http://dx.doi.org/10.1016/j.ijfatigue.2006.02.052.

[8] Fadaeifard F, Matori KA, Toozandehjani M, Daud AR, Ariffin MKAM, Othman NK, et al. Influence of rotational speed on mechanical properties of friction stir lap welded 6061-T6 Al alloy. Transactions of Nonferrous Metals Society of China. 2014;24(4):1004-1011. http://dx.doi.org/10.1016/S1003-6326(14)63155-1.

[9] Salari E, Jahazi M, Khodabandeh A, Ghasemi-Nanesa H. Influence of tool geometry and rotational speed on mechanical properties and defect formation in friction stir lap welded 5456 aluminum alloy sheets. Materials & Design. 2014;58:381-389. http://dx.doi.org/10.1016/j.matdes.2014.02.005.

[10] Salari E, Jahazi M, Khodabandeh A, Nanesa HG. Friction stir lap welding of 5456 aluminum alloy with different sheet thickness: process optimization and microstructure evolution. International Journal of Advanced Manufacturing Technology. 2016;82(1-4):39-48. http://dx.doi.org/10.1007/s00170-015-7342-5.

[11] Shirazi H, Kheirandish S, Safarkhanian MA. Effect of process parameters on the macrostructure and defect formation in friction stir lap welding of AA5456 aluminum alloy, measurement. Journal of the International Measurement Confederation. 2015;76:62-69. http://dx.doi.org/10.1016/j.measurement.2015.08.001.

[12] Yadava MK, Mishra RS, Chen YL, Carlson B, Grant GJ. Study of friction stir joining of thin aluminium sheets in lap joint configuration. Science and Technology of Welding and Joining. 2010;15(1):70-75. http://dx.doi.org/10.1179/136217109X12537145658733.

[13] Chen ZW, Yazdanian S. Friction Stir Lap Welding: material flow, joint structure and strength. Journal of Achievements in Materials and Manufacturing Engineering. 2012;55:629-637.

[14] Yazdanian S, Chen ZW, Littlefair G. Effects of friction stir lap welding parameters on weld features on advancing side and fracture strength of AA6060-T5 welds. Journal of Materials Science. 2012;47(3):1251-1261. http://dx.doi.org/10.1007/s10853-011-5747-6.

[15] Liu H, Hu Y, Peng Y, Dou C, Wang Z. The effect of interface defect on mechanical properties and its formation mechanism in friction stir lap welded joints of aluminium alloys. Journal of Materials Processing Technology. 2016;238:244-254. http://dx.doi.org/10.1016/j.jmatprotec.2016.06.029.

[16] Costa MI, Verdera D, Costa JD, Leitao C, Rodrigues DM. Influence of pin geometry and process parameters on friction stir lap welding of AA5754-H22 thin sheets. Journal of Materials Processing Technology. 2015;225:385-392. http://dx.doi.org/10.1016/j.jmatprotec.2015.06.020.

[17] Costa MI, Leitão C, Rodrigues DM. Influence of post-welding heat-treatment on the monotonic and fatigue strength of 6082-T6 friction stir lap welds. Journal of Materials Processing Technology. 2017;250:289-296. http://dx.doi.org/10.1016/j.jmatprotec.2017.07.030.

[18] Miller WS, Zhuang L, Bottema J, Wittebrood A, De Smet P, Haszler A, et al. Recent development in aluminium alloys for the automotive industry, Mat Sci. Engineering Structures. 2000;280:37-49.

[19] Fridlyander IN, Sister VG, Grushko OE, Berstenev VV, Sheveleva LM, Ivanova LA. Aluminum alloys: Promising materials in the automotive industry. Metal Science and Heat Treatment. 2002;44(9/10):365-370. http://dx.doi.org/10.1023/A:1021901715578.

[20] Leitão C, Galvão I, Leal RM, Rodrigues DM. Determination of local constitutive properties of aluminium friction stir welds using digital image correlation. Materials & Design. 2012;33:69-74. http://dx.doi.org/10.1016/j.matdes.2011.07.009.

[21] Leitão C, Costa MI, Khanijomdi K, Rodrigues DM. Assessing strength and local plastic behaviour of welds by shear testing. Materials & Design. 2013;51:968-974. http://dx.doi.org/10.1016/j.matdes.2013.04.100.

[22] Sato YS, Kokawa H, Enomoto M, Jogan S. Microstructural evolution of 6063 aluminum during friction- stir welding. Metallurgical and Materials Transactions A. 1999;30(9):2429-2437.

[23] Bozkurt Y, Salman S, Çam G. Effect of welding parameters on lap shear tensile properties of dissimilar friction stir spot welded AA 5754-H22/2024-T3 joints. Journal Science and Technology of Welding and Joining. 2013;18(4):337-345. https://doi.org/10.1179/1362171813Y.0000000111.